26th IMEKO TC4 International Symposium
24th International Workshop on ADC and DAC Modelling and Testing
IMEKO TC-4 2023
Pordenone, Italy / September 20-21, 2023

Rapid Prototyping of Automotive Magnetic Positioning Systems

Luiz G. Enger[1], Aleš Travnik[1], Peter Leitner[1], Florian Slanovc[1], Daniel Markó[1], Michael Ortner[1]

[1]*Silicon Austria Labs, Europastraße 12, 9524 Villach, Austria, luiz.enger@silicon-austria.com*

***Abstract* – Magnetic position and orientation systems offer the advantages of contactless sensing, high precision, robustness and low cost. They are heavily employed in automotive and industrial applications. The standard development process of such system starts with a simulation that is followed by validation with experimental data. This work presents a platform to which different sensors and magnets can be attached, with complete six degrees of freedom for relative movement. It is thus quite flexible in terms of experiments it can perform. A system calibration scheme based on dipole approximation is presented, yielding sensor tolerances and allowing to compute the field of a corresponding magnet.**

I. INTRODUCTION & MOTIVATION

Magnetic position and orientation (MPO) systems posses several advantages over other position and motion detection systems. They operate with contactless sensing, are thus wear-free and can work immersed in liquids such as motor oil [1]. They combine high-precision, robustness against moisture, dirt and temperature variations, and operate at low power consumption. Permanent magnets and magnetic field sensors are also relatively cheap thanks to large scale production. Due to these properties, MPO systems are extensively used in the automotive industry for engine and transmission control, pedal and steering wheel position sensing, anti-lock brake systems, active suspension and more [2, 3].

The general approach to develop a MPO system is to start with a simulation, followed by obtaining experimental data, which will be used for validation and to improve the simulation. Figure 1 shows common implementations of MPO systems, each requiring a specific setup to run experiments. There is no one-size-fits-all solution. To fill in this gap, a flexible platform to obtain precise experimental data which allows for rapid prototyping of MPO systems targeting automotive applications is proposed. Whereas some work has already been published using robot arms for linear movement and joystick applications or a Stewart platform holding an array of sensors for six degrees of freedom (6DoF) [5, 6, 7], this work presents a platform offering 6DoF with separated modules for translation and rotation movements.

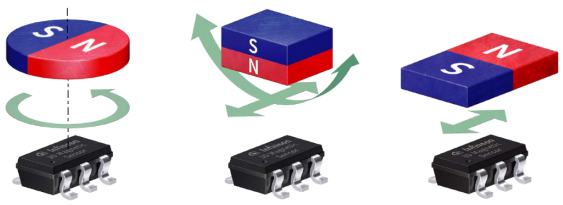

Fig. 1. Typical examples of MPO systems. From [4].

The major issue with magnetic position system testing equipment is the difficult alignment of position and orientation between sensor and magnet, which results from system assembly, but also imperfectly fabricated magnets and sensors themselves. Many schemes have been proposed to achieve such a calibration, all with their advantages and disadvantages [7, 8]. The proposed 6DoF setup requires a (semi-)automatic scheme, that will work with different magnets and sensors to enable fast prototyping and repeated measurements. In this work, we give an overview of the 6DoF setup and demonstrate a novel calibration scheme based on dipole field approximations.

II. PLATFORM FOR MPO PROTOTYPING

Our 6DoF test bench is mechanically designed to achieve a positioning precision of 100 µm, an angular precision of 0.1° while fully realizing 6DoF within a linear range of ±20 mm, and full 360° of rotation. The setup, shown in Fig. 2, consists of a 3D translation stage, onto which the sensor is mounted, and a 3D rotation stage the magnet is attached to. In combination, these two stages realize 6DoF motion. The majority of the pieces holding the test bench together are made from aluminum, since it is nonmagnetic, lightweight and easy to machine. Anodization of the parts was performed to provide a durable finish. The setup is mounted on a high-precision optical bread board, to provide the necessary stability. Each stage is independently controlled with a stepper motor, which in turn is controlled directly from a PC via a USB interface from a low-level Python back-end. The same back-end is used to obtain the sensor data, which allows for a high level of flexibility to operate with different sensors. In Fig. 2, an Infineon TLV493D-A1B6 MS2Go kit is mounted.

To achieve our mechanical precision goal, the mechanical deflection of fabricated components was calculated and accounted for together with fabrication tolerances and

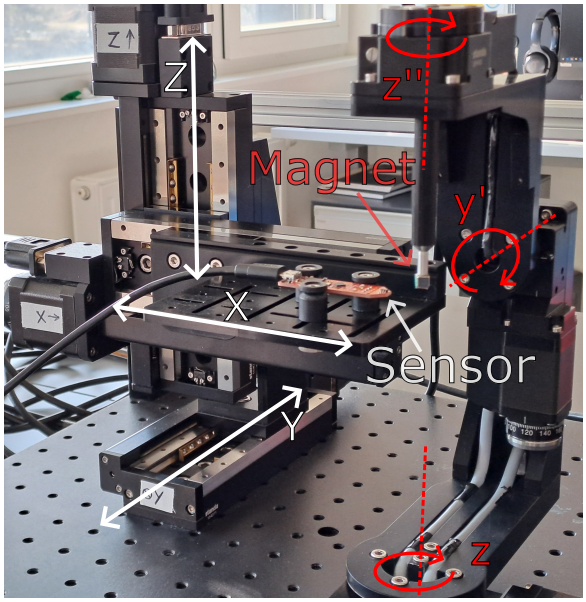

Fig. 2. Photo of the platform, with a sensor mounted onto the translation stage and a cube magnet attached to the tip of a shaft on the rotation stage. Translation axes are highlighted in white and rotation axes in red. Sensor and magnet are indicated.

assembly errors. The assembly of the test bench follows the left-hand convention, with the thumb pointing up towards positive Z-, straight index finger pointing towards positive Y- and middle finger pointing towards positive X-direction. The 3D rotation motion follows the z-y'-z'' convention for Euler angles considering intrinsic rotations. The 3D translation stage is constructed from three individual linear stages with a single step resolution of 2.5 µm. Like a goniometer, the 3D rotation stage itself is constructed from three individual rotation stages, where the z-rotation has 0.01° single step resolution, whereas y'- and z''- rotations can achieve 0.015° per step. The total range of motion for each translation axis is ±50 mm, and full 360° for the each rotation axis with no limit for the number of revolutions as slip-ring connectors are used to connect the stages.

The Python back-end forwards commands to the motor drivers to physically move the test bench. However, this back-end is not very convenient for purposes including complex relative motions between sensor and magnet. For defining relative paths between sensor and magnet, we make use of the practical Magpylib path standard [9]. A Python front-end translates a Magpylib path, possibly from a virtual experiment, into back-end commands that are needed to generate the desired motion in the experiment. To avoid collisions between individual components of the setup, e.g., between moving and resting stages or between sensor and magnet mounts, a digital twin of the setup was built with PyVista [10]. The digital twin can predict collisions based on given input parameters and allows only valid positions to be passed to the physical test bench.

III. CALIBRATION OF THE PLATFORM

To meet our target precision goal, all tolerances have to be identified, evaluated, and calibrated out. Tolerances can be divided into two main categories: (i) stage assembly tolerances and (ii) system assembly tolerances associated with every new experiment, including the tolerances of magnet, sensor(s) and their respective mounts.

A. *Stage calibration*

Manufacturing and assembly imperfections result in a set of critical errors including stage axes orthogonality, rotational eccentricity and runout. These errors lead to poor positioning and have to be accounted for. This is realized by precise characterization and subsequent correction when translating front-end paths to encoder signals.

For characterization of the test bench, a touch trigger probe model TPA2 is employed [11]. This probe triggers a signal whenever sufficient pressure is applied to its tip, either from the side or from below, with a repeatability of 2 µm. With this probe, the characterization of the above-mentioned tolerances is performed by touching the stages at various points of progress of individual motions.

B. *System calibration scheme*

While the stage tolerances are constants, every MPO system assembly introduces additional errors into the experiment. Those include intrinsic sensor and magnet tolerances like die position and orientation in package, sensing direction orthogonality, offset and gains, geometric imperfections and bad magnetization distributions. There are also tolerances related to how sensor and magnet are mounted onto the stage.

It is crucial for rapid prototyping to find a (semi-)automated calibration procedure with a high level of repeatability, that can, at the same time, flexibly deal with different magnets and sensors. We propose to exploit the fast decay of the magnetic field of higher order moments to find a good mechanical reference between sensor and magnet. In practice, the magnet is positioned at a distance from the sensor such that the latter is unable to distinguish between the magnet and a dipole field, but close enough so that variations can still be detected. A "sweet volume" corresponds to a shell around the sensor where both conditions are fulfilled. Its shape and size depend strongly on the magnet (shape and magnetization) and the sensor (resolution and range) properties.

The magnet is then moved along specific paths inside this "sweet volume" and magnetic field readings are stored.

An optimization algorithm subsequently performs a fit of the experimental data to the computed field values for a dipole source. The tolerances of interest are used as fitting parameters.

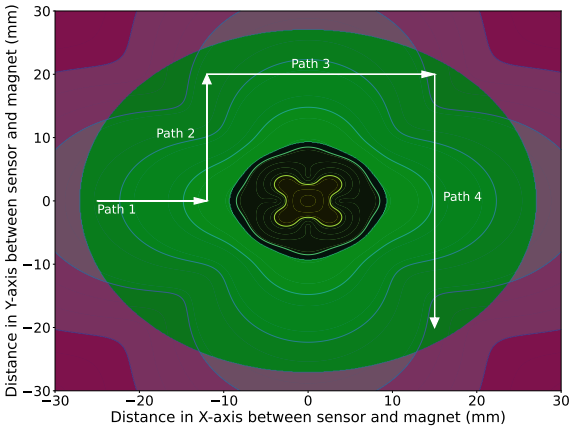

Fig. 3. Black zone: difference between dipole field and cube magnet field amplitudes is above sensor resolution. Red zone: field amplitude is below sensor resolution. Green zone: area in which the cube magnet can be effectively considered as a dipole, the sweet volume.

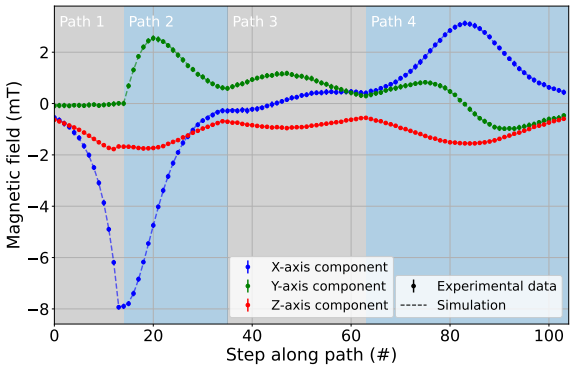

Fig. 4. Optimized dipole fit with average and standard deviation of 64 sensor readings at each position, with a step size of 1 mm.

C. Experimental calibration

For an ideal cube magnet of 5 mm long edges, magnetized in Z-direction with a remanence of 1000 mT and at an airgap of 5 mm from sensor, Fig. 3 shows the sweet volume of a TLV493D-A1B6 sensor at $Z = 0$ mm. A movement inside this volume is also defined, and Fig. 4 depicts the optimized fit between sensors readings and dipole field. Data was acquired using an off-the-shelf cube magnet.

A differential evolution algorithm was used [12, 13]. The optimization parameters were die position, orientation, sensitivity and offset as well as dipole moment for each XYZ component. After optimization, the maximum relative error in field amplitude amounts to 6.4% with an average of 2.0%. As the magnet was kept at a distance from the sensor, its field amplitude is smaller and stray fields have an increased effect on sensor readings. However, such effects were not taken into account for the evaluation of the sweet volume.

D. Proof of concept

A 1D linear motion MPO system was chosen to demonstrate the concept [5, 14]. Figure 5 displays the effective sweet volume after the dipole calibration. The optimized values of the dipole moment were used to calculate the magnetization of an equivalent cube magnet of 5 mm long edges. This has the drawback of considering a homogeneous magnetization and a perfect geometry for the magnet, and that the corresponding dipole is located at its center. The sensor Z position was also corrected. A linear path is defined, moving outside the sweet volume. With the same magnet previously used, sensor readings were obtained from $X = -16$ mm to $X = 16$ mm with a 1 mm step size. Figure 6 presents the comparison between experimental data and the calculated field of a cube magnet.

The maximum relative error in field amplitude was 15%. Differences between experiment and simulation arise outside the sweet volume as an ideal cube magnet was considered for field calculation. If information such as dimension and magnetization distribution is available from a previous magnet characterization, calculated field values will be closer to the experimental data. The presented scheme does not provide calibration of the magnet itself.

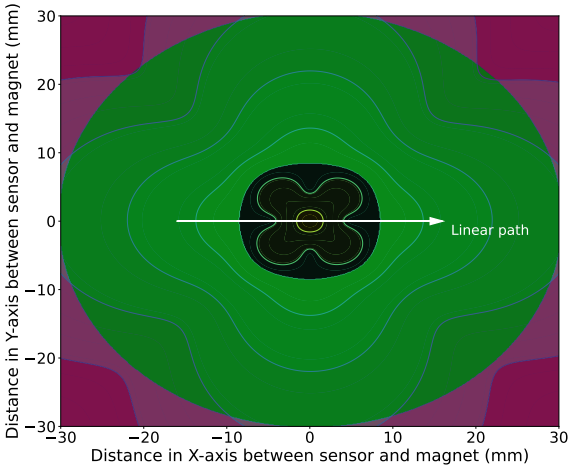

Fig. 5. Linear path crossing the region where sensor detects a difference between the field of a cube magnet and that of a dipole.

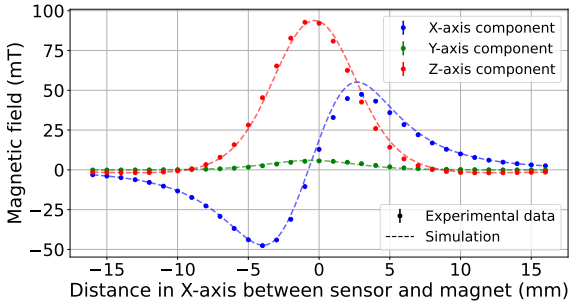

Fig. 6. Parameters from the optimized fit of a dipole field were used to calculate the field of a cube magnet.

IV. CONCLUSION

Positioning systems based on magnetic field sensing of a permanent magnet present several advantages over other systems such as low cost, low power consumption, robustness against hazardous environments and are wear-free due to contactless sensing. This work presented the assembly and discussed the calibration of a platform with six degrees of freedom movement, capable of reproducing every possible relative position and motion between a magnetic field sensor and a permanent magnet. Special attention was given to a system calibration scheme based on a dipole field approximation. This scheme yields the tolerances of the magnetic sensor in a MPO system and the corresponding dipole moment values of a magnet moving inside a sweet volume. Those results can be used to calculate the actual magnetic field of the magnet, although the error increases outside the sweet volume as a magnet with ideal geometry and magnetization distribution is considered. The calibration can be further improved with data obtained from the characterization of the magnet itself and by taking into account other effects such as from stray fields.

REFERENCES

[1] Joseph P. Heremans. "Magnetic Field Sensors for Magnetic Position Sensing in Automotive Applications". In: *MRS Online Proceedings Library* 475.1 (Dec. 1997), pp. 63–74. ISSN: 1946-4274. DOI: 10.1557/PROC-475-63. URL: https://doi.org/10.1557/PROC-475-63.

[2] C.P.O Treutler. "Magnetic sensors for automotive applications". In: *Sensors and Actuators A: Physical* 91.1 (2001). Third European Conference on Magnetic Sensors & Actuators., pp. 2–6. ISSN: 0924-4247. DOI: https://doi.org/10.1016/S0924-4247(01)00621-5. URL: https://www.sciencedirect.com/science/article/pii/S0924424701006215.

[3] Udo Ausserlechner, Armin Satz and Ferdinand Gastinger. *Magnetic position sensors, systems and methods*. US11287252B2. Sept. 2020. URL: https://patents.google.com/patent/US11287252B2/.

[4] Infineon Technologies AG. *XENSIV™ - sensing the world*. Nov. 2022.

[5] Michael Ortner, Marcelo Ribeiro and Dietmar Spitzer. "Absolute Long-Range Linear Position System With a Single 3-D Magnetic Field Sensor". In: *IEEE Transactions on Magnetics* 55.1 (2019), pp. 1–4. DOI: 10.1109/TMAG.2018.2870597.

[6] Perla Malagò et al. "Magnetic Position System Design Method Applied to Three-Axis Joystick Motion Tracking". In: *Sensors* 20.23 (2020). ISSN: 1424-8220. DOI: 10.3390/s20236873. URL: https://www.mdpi.com/1424-8220/20/23/6873.

[7] Daniel Cichon et al. "A Hall-Sensor-Based Localization Method With Six Degrees of Freedom Using Unscented Kalman Filter". In: *IEEE Sensors Journal* 19.7 (2019), pp. 2509–2516. DOI: 10.1109/JSEN.2018.2887299.

[8] Stefano Lumetti et al. "Computationally Efficient Magnetic Position System Calibration". In: *Engineering Proceedings* 2.1 (2020). ISSN: 2673-4591. DOI: 10.3390/ecsa-7-08219. URL: https://www.mdpi.com/2673-4591/2/1/72.

[9] Michael Ortner and Lucas Gabriel Coliado Bandeira. "Magpylib: A free Python package for magnetic field computation". In: *SoftwareX* (2020). DOI: 10.1016/j.softx.2020.100466.

[10] Bane Sullivan and Alexander Kaszynski. "PyVista: 3D plotting and mesh analysis through a streamlined interface for the Visualization Toolkit (VTK)". In: *Journal of Open Source Software* 4.37 (May 2019), p. 1450. DOI: 10.21105/joss.01450. URL: https://doi.org/10.21105/joss.01450.

[11] Kurokesu. *TPA2*. URL: https://wiki.kurokesu.com/books/tpa2 (visited on 30/03/2023).

[12] Pauli Virtanen et al. "SciPy 1.0: fundamental algorithms for scientific computing in Python". In: *Nature Methods* 17.3 (Feb. 2020), pp. 261–272. DOI: 10.1038/s41592-019-0686-2.

[13] Rainer Storn and Kenneth Price. In: *Journal of Global Optimization* 11.4 (1997), pp. 341–359. DOI: 10.1023/a:1008202821328.

[14] Florian Slanovc, Dieter Suess and Michael Ortner. "Designing Airgap-Stable Magnetic Linear Position Systems". In: *IEEE Transactions on Magnetics* 58.9 (2022), pp. 1–5. DOI: 10.1109/TMAG.2022.3188474.